Symplectic Solution for Size-dependent Contact Analysis

Lizichen Chen[a], Weiqiu Chen[a,b,c,*]

[a]*Key Laboratory of Soft Machines and Smart Devices of Zhejiang Province, Department of Engineering Mechanics, Soft Matter Research Center, Zhejiang University, Hangzhou 310027, P.R. China*

[b]*Center for Soft Machines and Smart Devices, Huanjiang Laboratory, Zhuji 311816, P.R. China*

[c]*Faculty of Mechanical Engineering and Mechanics, Ningbo University, Ningbo 315211, P.R. China*

Abstract

A novel symplectic framework suitable for size-dependent contact analysis has been established. The governing equations in symplectic form are derived for the contact between a no-slip rigid punch and a finite-sized plane with horizontal exponential material gradient. The dual Hamiltonian transformation of a quasi-Hamiltonian operator with asymmetric lower-left block is constructed. All the eigen-solutions are obtained analytically, which lead to the derivation of the coefficients in symplectic expansion via Hamiltonian mixed energy variational principle. The unique formulations of the symplectic expansion fundamentally stem from the distributions of the eigenvalues. Local phase transition is observed and analyzed, revealing that the size effect originates from the existence of real eigenvalues. A typical numerical example is given to present the efficiency of the symplectic approach, which lays the theoretical foundation for material characterization utilizing high-throughput testing methodologies and functionally graded specimens.

Keywords: Symplectic framework; Size-dependent contact analysis; Horizontal exponential gradient; Quasi-Hamiltonian operator; Local phase transition

* *Corresponding author.* Tel./Fax: 85-571-87951866; *E-mail:* chenwq@zju.edu.cn. (Weiqiu Chen)

1. Introduction

Extensive researches into materials at the micro- and nano-scales [1,2] have not only unveiled the unique properties of specimens but have also significantly propelled the miniaturization of devices. For instance, micro-electro-mechanical system (MEMS) is a representative device, as the unique size-dependent effects and surface effects critically influence its mechanical properties, necessitating more meticulous considerations in design and application [3]. Moreover, numerous micro-scale friction and contact issues arise during the operation of MEMS [4], posing challenges to stability and reliability of the system. To better understand material properties at the micro- and nano-scales and predict its special mechanical behaviors, many scholars have developed higher-order continuum mechanics models such as couple stress theory [5-7] and nonlocal theory [8] by introducing new internal material parameters [9]. The presence of couple stresses results in the asymmetric Cauchy stress tensors, and the reciprocal theorem of shear stresses no longer holds. Yang et al. [10] then established a modified couple stress theory for isotropic materials by neglecting the antisymmetric component.

In theoretical analysis, methods such as integral transform and Green's function approach are commonly employed. Notably, Muki and Sternberg [11] studied the response of flat punch indentation in couple-stress case by dual integral equations. Zisis and his collaborators summarized some fundamental techniques two-dimensional contact problems with couple stress model, investigating frictionless contact problems of a homogeneous elastic half-plane under a rigid indenter in plane-strain state [12], complete and receding contact problems with tilted flat punch [13], frictionless contact problems under cylindrical and wedge indenters [14], and contact problems in a layered system [15-16]. In terms of multi-field coupling, they also explored the

thermoelastic contact problem with a flat indenter [17]. Wang and his collaborators focused on three-dimensional spherical rigid indenters, analyzing the impact of material characteristic length, Poisson's ratio, and film thickness on contact behaviors [18-19]. Experimentally, guided by the micro- and nano-contact mechanics, advanced instruments such as nanoindentors and atomic force microscopes (AFM) have emerged [20-21]. These instruments play a crucial role in characterizing material performance, measuring parameters such as elastic modulus, hardness, and fracture toughness [22].

Nevertheless, there are limited researches on the size-dependent contact analysis which focus on inhomogeneous media. The inherent complexity facilitates us to devise a novel framework to address the obstacle. Zhong has proposed a symplectic method [23-24] for elasticity and generalized it to a model that suitable for couple stress case [25], which involves three Mindlin stress functions and its corresponding strain as dual variables. However, this formulation is not efficient for the contact analysis which featured by the mixed boundary conditions.

A novel symplectic framework for the contact analysis of a no-slip rigid punch acting on the surface of a finite-sized plane with exponential material gradient in the horizontal direction is constructed in this article. The dual Hamiltonian transformation of a quasi-Hamiltonian operator is derived via the governing equations in symplectic form. Zero eigenvalue and general eigenvalues along with the corresponding eigen-solutions are established analytically in Sections 2.1 and 2.2, respectively, which facilitate the introduction of symplectic expansion for complete set of solutions in Section 2.3. The local phase transition observed in the distributions of the eigenvalues is analyzed in Section 3.1, which interprets the phenomenon of size effect. A simple

numerical example is displayed in Section 3.2. The concluding remarks are given in Section 4.

2. Theoretical formulations

Considering a flat punch is applied on the surface of the functionally graded plane, as displayed in Fig. 1. The plane is isotropic, with E, ν, and ℓ being the Young's modulus, Poisson's ratio, and material characteristic length, respectively. We assume that E varies exponentially along the x-direction: $E(x)=E_0\mathrm{e}^{\beta x}$, and the rest keep constant, where E_0 represents Young's modulus at the coordinate origin; β is the material gradient index.

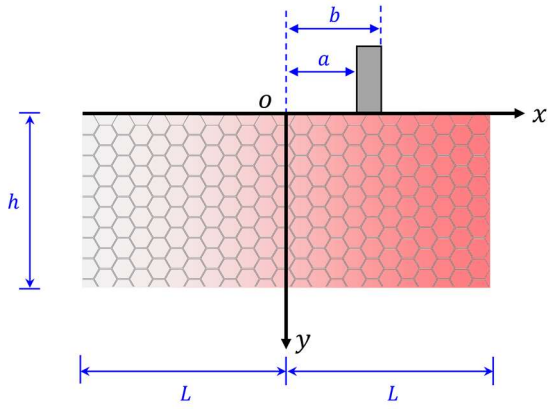

Fig. 1. A flat punch acting on the surface of a horizontally graded plane.

The two-dimensional constitutive equations for the plane strain case are in the form of:

$$\begin{cases} \varepsilon_{xx}=\dfrac{\partial u_x}{\partial x}=\dfrac{1+\nu}{E}\left[(1-\nu)\sigma_{xx}-\nu\sigma_{yy}\right] \\ \varepsilon_{yy}=\dfrac{\partial u_y}{\partial y}=\dfrac{1+\nu}{E}\left[(1-\nu)\sigma_{yy}-\nu\sigma_{xx}\right] \\ \varepsilon_{xy}=\varepsilon_{yx}=\dfrac{1}{2}\left(\dfrac{\partial u_x}{\partial y}+\dfrac{\partial u_y}{\partial x}\right)=\dfrac{1+\nu}{2E}\left(\sigma_{xy}+\sigma_{yx}\right) \\ \chi_{xz}=\dfrac{\partial \omega_z}{\partial x}=\dfrac{1}{2}\dfrac{\partial}{\partial x}\left(\dfrac{\partial u_y}{\partial x}-\dfrac{\partial u_x}{\partial y}\right)=\dfrac{1+\nu}{2E\ell^2}m_{xz} \\ \chi_{yz}=\dfrac{\partial \omega_z}{\partial y}=\dfrac{1}{2}\dfrac{\partial}{\partial y}\left(\dfrac{\partial u_y}{\partial x}-\dfrac{\partial u_x}{\partial y}\right)=\dfrac{1+\nu}{2E\ell^2}m_{yz} \end{cases} \tag{1}$$

where σ_{ij}, ε_{ij}, m_{ij}, and χ_{ij} are the stress, strain, couple stress, and curvature components,

respectively; u_x and u_y are the displacement components in the x- and y-directions, respectively; ω_z is the rotation vector in the normal direction. We may rearrange Eq. (1) and the equilibrium equations without body terms in the form of:

$$\begin{cases} \dfrac{\partial u_x}{\partial y}=\dfrac{\partial u_y}{\partial x}-2\omega_z \\ \dfrac{\partial u_y}{\partial y}=\dfrac{1+\nu}{E}\left[(1-\nu)\sigma_{yy}-\nu\sigma_{xx}\right] \\ \dfrac{\partial \omega_z}{\partial y}=\dfrac{1+\nu}{2E\ell^2}m_{yz} \\ \dfrac{\partial \sigma_{yx}}{\partial y}=-\dfrac{\partial \sigma_{xx}}{\partial x} \\ \dfrac{\partial \sigma_{yy}}{\partial y}=-\dfrac{\partial \sigma_{xy}}{\partial x} \\ \dfrac{\partial m_{yz}}{\partial y}=-\dfrac{\partial m_{xz}}{\partial x}+\sigma_{yx}-\sigma_{xy} \end{cases} \tag{2}$$

which are further simplified by introducing $\hat{\sigma}_{ij}=\sigma_{ij}\mathrm{e}^{-\beta x}$ and $\hat{m}_{ij}=m_{ij}\mathrm{e}^{-\beta x}$:

$$\frac{\partial}{\partial y}\mathbf{I}_6\boldsymbol{f}=\boldsymbol{\mathcal{H}}\boldsymbol{f} \tag{3}$$

where $\mathbf{I}_n$ is a nth-order identity matrix; $\boldsymbol{f}=[\boldsymbol{q},\boldsymbol{p}]^{\mathrm{T}}=[u_x,u_y,\omega_z,\hat{\sigma}_{yx},\hat{\sigma}_{yy},\hat{m}_{yz}]^{\mathrm{T}}$ is the full state vector; $\boldsymbol{\mathcal{H}}$ is a quasi-Hamiltonian operator:

$$\boldsymbol{\mathcal{H}}=\left[\begin{array}{ccc|ccc} 0 & \dfrac{\partial}{\partial x} & -2 & 0 & 0 & 0 \\ -\dfrac{\nu}{1-\nu}\dfrac{\partial}{\partial x} & 0 & 0 & 0 & \dfrac{(1+\nu)(1-2\nu)}{E_0(1-\nu)} & 0 \\ 0 & 0 & 0 & 0 & 0 & \dfrac{1+\nu}{2E_0\ell^2} \\ \hline -\dfrac{E_0}{1-\nu^2}\left(\dfrac{\partial^2}{\partial x^2}+\beta\dfrac{\partial}{\partial x}\right) & 0 & 0 & 0 & -\dfrac{\nu}{1-\nu}\left(\dfrac{\partial}{\partial x}+\beta\right) & 0 \\ 0 & -\dfrac{2E_0}{1+\nu}\left(\dfrac{\partial^2}{\partial x^2}+\beta\dfrac{\partial}{\partial x}\right) & \dfrac{2E_0}{1+\nu}\left(\dfrac{\partial}{\partial x}+\beta\right) & \left(\dfrac{\partial}{\partial x}+\beta\right) & 0 & 0 \\ 0 & -\dfrac{2E_0}{1+\nu}\dfrac{\partial}{\partial x} & -\dfrac{2E_0\ell^2}{1+\nu}\left(\dfrac{\partial^2}{\partial x^2}+\beta\dfrac{\partial}{\partial x}\right)+\dfrac{2E_0}{1+\nu} & 2 & 0 & 0 \end{array}\right]$$

from which we may assume $\boldsymbol{\mathcal{H}}=\left[\begin{array}{c|c}\mathbf{A} & \mathbf{B}\\ \hline \mathbf{C} & \mathbf{D}\end{array}\right]$, then $\mathbf{A}=-\lim\limits_{\beta\to 0}\mathbf{D}^{\mathcal{T}}$, $\mathbf{B}=\mathbf{B}^{\mathcal{T}}$, and $\lim\limits_{\beta\to 0}\mathbf{C}=\lim\limits_{\beta\to 0}\mathbf{C}^{\mathcal{T}}$ (i.e., $\mathbf{C}\neq\mathbf{C}^{\mathrm{T}}$), where $(\cdot)^{\mathcal{T}}$ represents the adjoint transpose of an operator matrix. Additionally, the

supplementary equations are derived to be

$$\hat{\sigma}_{xy}=\frac{2E_0}{1+\nu}\left(\frac{\partial u_y}{\partial x}-\omega_z\right)-\hat{\sigma}_{yx},\quad \hat{\sigma}_{xx}=\frac{E_0}{1-\nu^2}\frac{\partial u_x}{\partial x}+\frac{\nu}{1-\nu}\hat{\sigma}_{yy},\quad \hat{m}_{xz}=\frac{2E_0\ell^2}{1+\nu}\frac{\partial \omega_z}{\partial x} \tag{4}$$

Furthermore, the dual Hamiltonian transformation is proved through integration by parts, together with the homogeneous boundary conditions at $x=\pm L:\ \hat{\sigma}_{xy}=0$, $\hat{\sigma}_{xx}=0$, and $\hat{m}_{xz}=0$, which reads

$$\left\langle \boldsymbol{f}_1,\boldsymbol{\mathcal{H}}\boldsymbol{f}_2\right\rangle=\left\langle \boldsymbol{f}_2,\boldsymbol{\mathcal{H}}\boldsymbol{f}_1\right\rangle-\beta\left\langle \boldsymbol{f}_1^*,\boldsymbol{f}_2^*\right\rangle \tag{5}$$

where the subscript 1 or 2 denotes a specified state vector; $\boldsymbol{f}^*=[u_x,u_y,\omega_z,\hat{\sigma}_{xx},\hat{\sigma}_{xy},\hat{m}_{xz}]^{\mathrm{T}}$ is the dual full state vector, and the symplectic inner product is defined as

$$\left\langle \boldsymbol{f}_1,\boldsymbol{f}_2\right\rangle=\int_{-L}^{L}\boldsymbol{f}_1^{\mathrm{T}}\mathbf{J}\boldsymbol{f}_2\mathrm{d}x=\int_{-L}^{L}(u_{x1}\hat{\sigma}_{yx2}+u_{y1}\hat{\sigma}_{yy2}+\omega_{z1}\hat{m}_{yz2}-\hat{\sigma}_{yx1}u_{x2}-\hat{\sigma}_{yy1}u_{y2}-\hat{m}_{yz1}\omega_{z2})\mathrm{d}x \tag{6}$$

where $\mathbf{J}$ is unit symplectic matrix

$$\mathbf{J}=\begin{bmatrix}0 & \mathbf{I}_3\\ -\mathbf{I}_3 & 0\end{bmatrix} \tag{7}$$

The following expression is adopted for separation of variables:

$$\boldsymbol{f}(x,y)=\boldsymbol{\Phi}(x)\xi(y)=[u_x(x),u_y(x),\omega_z(x),\hat{\sigma}_{yx}(x),\hat{\sigma}_{yy}(x),\hat{m}_{yz}(x)]^{\mathrm{T}}\xi(y) \tag{8}$$

Substituting Eq. (8) into Eq. (3) yields

$$\frac{\dfrac{\partial}{\partial y}\xi(y)}{\xi(y)}=[\boldsymbol{\mathcal{H}}\boldsymbol{\Phi}(x)]\boldsymbol{\Phi}^{-1}(x) \tag{9}$$

which leads to

$$\xi(y)=\mathrm{e}^{\mu y} \tag{10}$$

and the eigen equation

$$\boldsymbol{\mathcal{H}}\boldsymbol{\Phi}(x)=\mu\boldsymbol{\Phi}(x) \tag{11}$$

where μ is the eigenvalue, and $\boldsymbol{\Phi}(x)$ is the corresponding eigenvector.

2.1. Eigen-solutions of zero eigenvalue

Due to the stress-free boundary conditions, the eigen-solutions for zero eigenvalue exist, which constitute the Saint-Venant solutions. It is interesting to note that Eq. (10) is rewritten as $\xi(y)=1$ under the case of the zero eigenvalue, which indicates the decaying terms along the y-axis vanish. The governing equations are detailed as

$$\begin{cases} \dfrac{\mathrm{d}u_y(x)}{\mathrm{d}x}-2\omega_z(x)=0 \\ -\dfrac{\nu}{1-\nu}\dfrac{\mathrm{d}u_x(x)}{\mathrm{d}x}+\dfrac{(1+\nu)(1-2\nu)}{E_0(1-\nu)}\hat{\sigma}_{yy}(x)=0 \\ \dfrac{1+\nu}{2E_0\ell^2}\hat{m}_{yz}(x)=0 \\ -\dfrac{E_0}{1-\nu^2}\dfrac{\mathrm{d}^2u_x(x)}{\mathrm{d}x^2}-\dfrac{\nu}{1-\nu}\dfrac{\mathrm{d}\hat{\sigma}_{yy}(x)}{\mathrm{d}x}-\beta\left(\dfrac{E_0}{1-\nu^2}\dfrac{\mathrm{d}u_x(x)}{\mathrm{d}x}+\dfrac{\nu}{1-\nu}\hat{\sigma}_{yy}(x)\right)=0 \\ -\dfrac{2E_0}{1+\nu}\left(\dfrac{\mathrm{d}^2u_y(x)}{\mathrm{d}x^2}-\dfrac{\mathrm{d}\omega_z(x)}{\mathrm{d}x}\right)+\dfrac{\mathrm{d}\hat{\sigma}_{yx}(x)}{\mathrm{d}x}-\beta\left[\dfrac{2E_0}{1+\nu}\left(\dfrac{\mathrm{d}u_y(x)}{\mathrm{d}x}-\omega_z(x)\right)-\hat{\sigma}_{yx}(x)\right]=0 \\ -\dfrac{2E_0\ell^2}{1+\nu}\dfrac{\mathrm{d}^2\omega_z(x)}{\mathrm{d}x^2}-\beta\dfrac{2E_0\ell^2}{1+\nu}\dfrac{\mathrm{d}\omega_z(x)}{\mathrm{d}x}+\dfrac{2E_0}{1+\nu}\omega_z(x)+2\hat{\sigma}_{yx}(x)-\dfrac{2E_0}{1+\nu}\dfrac{\mathrm{d}u_y(x)}{\mathrm{d}x}=0 \end{cases} \tag{12}$$

The eigenvectors are obtained under the homogeneous boundary conditions as

$$\boldsymbol{f}_{0,1}^{(0)}=\boldsymbol{\Phi}_{0,1}^{(0)}=[1,0,0,0,0,0]^{\mathrm{T}},\quad \boldsymbol{f}_{0,2}^{(0)}=\boldsymbol{\Phi}_{0,2}^{(0)}=[0,1,0,0,0,0]^{\mathrm{T}} \tag{13}$$

where the superscript $(\cdot)$ represents the order of Jordan form, and the subscript $0,i$ represents the i-th Jordan chain for zero eigenvalue. It is important to emphasize that the eigenvectors and the corresponding eigen-solutions in Eq. (13) share common expressions, respectively. The first-order Jordan form eigenvectors of zero eigenvalue are

$$\boldsymbol{\mathcal{H}}\boldsymbol{\Phi}_{0,1}^{(1)}=\boldsymbol{\Phi}_{0,1}^{(0)},\quad \boldsymbol{\mathcal{H}}\boldsymbol{\Phi}_{0,2}^{(1)}=\boldsymbol{\Phi}_{0,2}^{(0)} \tag{14}$$

from which we may obtain

$$\boldsymbol{\Phi}_{0,1}^{(1)}=[0,-x,-1,0,0,0]^{\mathrm{T}},\quad \boldsymbol{\Phi}_{0,2}^{(1)}=[-\frac{\nu}{1-\nu}x,0,0,0,\frac{E_0}{1-\nu^2},0]^{\mathrm{T}} \tag{15}$$

and the corresponding eigen-solutions for the first-order are established as

$$\boldsymbol{f}_{0,1}^{(1)}=\boldsymbol{\Phi}_{0,1}^{(1)}+y\boldsymbol{\Phi}_{0,1}^{(0)}=[y,-x,-1,0,0,0]^{\mathrm{T}},\quad \boldsymbol{f}_{0,2}^{(1)}=\boldsymbol{\Phi}_{0,2}^{(1)}+y\boldsymbol{\Phi}_{0,2}^{(0)}=[-\frac{\nu}{1-\nu}x,y,0,0,\frac{E_0}{1-\nu^2},0]^{\mathrm{T}} \tag{16}$$

By analogizing the aforementioned formula, the second-order Jordan form eigen equations are constructed accordingly:

$$\boldsymbol{\mathcal{H}}\boldsymbol{\Phi}_{0,1}^{(2)}=\boldsymbol{\Phi}_{0,1}^{(1)},\quad \boldsymbol{\mathcal{H}}\boldsymbol{\Phi}_{0,2}^{(2)}=\boldsymbol{\Phi}_{0,2}^{(1)} \tag{17}$$

the first equation is solved for the eigenvector

$$\boldsymbol{\Phi}_{0,1}^{(2)}=[\frac{1}{2}\frac{\nu}{1-\nu}x^2,0,0,0,-\frac{E_0}{1-\nu^2}x,-\frac{2E_0\ell^2}{1+\nu}]^{\mathrm{T}} \tag{18}$$

However, no practical eigenvector satisfies the second equation of Eq. (17), which indicates the termination of the Jordan chain. Subsequently, the eigen-solution for the first chain is deduced as

$$\boldsymbol{f}_{0,1}^{(2)}=\boldsymbol{\Phi}_{0,1}^{(2)}+y\boldsymbol{\Phi}_{0,1}^{(1)}+\frac{y^2}{2}\boldsymbol{\Phi}_{0,1}^{(0)}=[\frac{1}{2}\left(\frac{\nu}{1-\nu}x^2+y^2\right),-xy,-y,0,-\frac{E_0}{1-\nu^2}x,-\frac{2E_0\ell^2}{1+\nu}]^{\mathrm{T}} \tag{19}$$

Concerning the absence of the third-order Jordan form eigenvector, we may set

$$\boldsymbol{\Phi}_0^{(2)}=\boldsymbol{\Phi}_{0,1}^{(2)}+\zeta_0\boldsymbol{\Phi}_{0,2}^{(1)} \tag{20}$$

where ζ_0 is a constant. Following the same procedure as for Eq. (17)

$$\boldsymbol{\mathcal{H}}\boldsymbol{\Phi}_0^{(3)}=\boldsymbol{\Phi}_0^{(2)} \tag{21}$$

which is detailed as

$$\begin{cases}
\dfrac{\mathrm{d}u_y(x)}{\mathrm{d}x}-2\omega_z(x)=\dfrac{\nu}{1-\nu}\left(\dfrac{1}{2}x^2-\zeta_0 x\right)\\
-\dfrac{\nu}{1-\nu}\dfrac{\mathrm{d}u_x(x)}{\mathrm{d}x}+\dfrac{(1+\nu)(1-2\nu)}{E_0(1-\nu)}\hat{\sigma}_{yy}(x)=0\\
\dfrac{1+\nu}{2E_0\ell^2}\hat{m}_{yz}(x)=0\\
-\dfrac{E_0}{1-\nu^2}\dfrac{\mathrm{d}^2u_x(x)}{\mathrm{d}x^2}-\dfrac{\nu}{1-\nu}\dfrac{\mathrm{d}\hat{\sigma}_{yy}(x)}{\mathrm{d}x}-\beta\left(\dfrac{E_0}{1-\nu^2}\dfrac{\mathrm{d}u_x(x)}{\mathrm{d}x}+\dfrac{\nu}{1-\nu}\hat{\sigma}_{yy}(x)\right)=0\\
-\dfrac{2E_0}{1+\nu}\left(\dfrac{\mathrm{d}^2u_y(x)}{\mathrm{d}x^2}-\dfrac{\mathrm{d}\omega_z(x)}{\mathrm{d}x}\right)+\dfrac{\mathrm{d}\hat{\sigma}_{yx}(x)}{\mathrm{d}x}-\beta\left[\dfrac{2E_0}{1+\nu}\left(\dfrac{\mathrm{d}u_y(x)}{\mathrm{d}x}-\omega_z(x)\right)-\hat{\sigma}_{yx}(x)\right]=-\dfrac{E_0}{1-\nu^2}(x-\zeta_0)\\
-\dfrac{2E_0\ell^2}{1+\nu}\dfrac{\mathrm{d}^2\omega_z(x)}{\mathrm{d}x^2}-\beta\dfrac{2E_0\ell^2}{1+\nu}\dfrac{\mathrm{d}\omega_z(x)}{\mathrm{d}x}+\dfrac{2E_0}{1+\nu}\omega_z(x)+2\hat{\sigma}_{yx}(x)-\dfrac{2E_0}{1+\nu}\dfrac{\mathrm{d}u_y(x)}{\mathrm{d}x}=-\dfrac{2E_0\ell^2}{1+\nu}
\end{cases} \tag{22}$$

We therefore get ζ_0 through the analysis of the fifth equation of Eq. (22) with the homogeneous boundary conditions at $x=\pm L$:

$$\frac{2E_0}{1+\nu}\left(\frac{\partial u_y(x)}{\partial x}-\omega_z(x)\right)-\hat{\sigma}_{yx}(x)=c_1\mathrm{e}^{-\beta x}+\frac{E_0}{\beta^2(1-\nu^2)}(x\beta-\beta\zeta_0-1) \tag{23}$$

where

$$\begin{cases}\zeta_0=-\dfrac{1}{\beta}+L\coth(\beta L)\\ c_1=\dfrac{E_0 L\,\mathrm{csch}(\beta L)}{\beta(1-\nu^2)}\end{cases} \tag{24}$$

from which we arrive at

$$\boldsymbol{\Phi}_0^{(3)}=[0,\psi_1,\psi_2,\psi_3,0,0]^{\mathrm{T}} \tag{25}$$

and the respective eigen-solution:

$$\boldsymbol{f}_0^{(3)}=\boldsymbol{\Phi}_0^{(3)}+y\boldsymbol{\Phi}_{0,1}^{(2)}+\frac{y^2}{2!}\boldsymbol{\Phi}_{0,1}^{(1)}+\frac{y^3}{3!}\boldsymbol{\Phi}_{0,1}^{(0)}+\zeta_0 y\boldsymbol{\Phi}_{0,2}^{(1)}+\zeta_0\frac{y^2}{2!}\boldsymbol{\Phi}_{0,2}^{(0)} \tag{26}$$

where

$$\begin{cases}\psi_1=2\dfrac{\phi_1}{\lambda_1}\mathrm{e}^{\lambda_1 x}+2\dfrac{\phi_2}{\lambda_1}\mathrm{e}^{\lambda_2 x}\\ \quad -\dfrac{1}{\beta(1-\nu)}\left[\dfrac{L\,\mathrm{csch}(\beta L)}{\beta}\mathrm{e}^{-\beta x}+\left(\dfrac{\beta\nu}{3}x^3+\dfrac{\theta_1}{2}x^2+\theta_0 x\right)\right]+\dfrac{\nu}{1-\nu}\left(\dfrac{1}{6}x^3-\dfrac{\zeta_0}{2}x^2\right)\\ \psi_2=\phi_1\mathrm{e}^{\lambda_1 x}+\phi_2\mathrm{e}^{\lambda_2 x}+\dfrac{1}{2\beta(1-\nu)}\left[L\,\mathrm{csch}(\beta L)\mathrm{e}^{-\beta x}-\left(\beta\nu x^2+\theta_1 x+\theta_0\right)\right]\\ \psi_3=\dfrac{2E_0}{1+\nu}\left\{\phi_1\mathrm{e}^{\lambda_1 x}+\phi_2\mathrm{e}^{\lambda_2 x}+\dfrac{1}{2\beta(1-\nu)}\left[L\,\mathrm{csch}(\beta L)\mathrm{e}^{-\beta x}-\left(\beta\nu x^2+\theta_1 x+\theta_0\right)\right]\right\}\\ \quad +\dfrac{2E_0\nu}{1-\nu^2}\left(\dfrac{1}{2}x^2-\zeta_0 x\right)-\dfrac{E_0}{\beta(1-\nu^2)}\left[x-L\coth(\beta L)+L\,\mathrm{csch}(\beta L)\mathrm{e}^{-\beta x}\right]\end{cases} \tag{27}$$

where

$$\begin{cases}\lambda_1=\dfrac{-\beta\ell+\sqrt{\beta^2\ell^2+4}}{2\ell}\\ \lambda_2=-\dfrac{\beta\ell+\sqrt{\beta^2\ell^2+4}}{2\ell}\\ \theta_1=2\nu-1+2\ell^2\beta^2\nu-2L\beta\nu\coth(\beta L)\\ \theta_0=\ell^2\beta(1+2\nu+2\ell^2\beta^2\nu)+L\coth(\beta L)-2L\beta^2\ell^2\nu\coth(\beta L)\\ \phi_1=\dfrac{2\beta L\nu\cosh(\lambda_2 L)-\beta L\,\mathrm{csch}(\beta L)\sinh[(\beta+\lambda_2)L]-\theta_1\sinh(\lambda_2 L)}{2\beta\lambda_1(1-\nu)\sinh[(\lambda_1-\lambda_2)L]}\\ \phi_2=\dfrac{2\beta L\nu\cosh(\lambda_1 L)-\beta L\,\mathrm{csch}(\beta L)\sinh[(\beta+\lambda_1)L]-\theta_1\sinh(\lambda_1 L)}{2\beta\lambda_2(1-\nu)\sinh[(\lambda_2-\lambda_1)L]}\end{cases} \tag{28}$$

2.2. Eigen-solutions of general eigenvalues

The eigen equation is constructed according to Eq. (11), which yields

$$\begin{cases} \dfrac{\mathrm{d}u_y(x)}{\mathrm{d}x} - 2\omega_z(x) = \mu u_x(x) \\ -\dfrac{\nu}{1-\nu}\dfrac{\mathrm{d}u_x(x)}{\mathrm{d}x} + \dfrac{(1+\nu)(1-2\nu)}{E_0(1-\nu)}\hat{\sigma}_{yy}(x) = \mu u_y(x) \\ \dfrac{1+\nu}{2E_0\ell^2}\hat{m}_{yz}(x) = \mu\omega_z(x) \\ -\dfrac{E_0}{1-\nu^2}\dfrac{\mathrm{d}^2u_x(x)}{\mathrm{d}x^2} - \dfrac{\nu}{1-\nu}\dfrac{\mathrm{d}\hat{\sigma}_{yy}(x)}{\mathrm{d}x} - \beta\left(\dfrac{E_0}{1-\nu^2}\dfrac{\mathrm{d}u_x(x)}{\mathrm{d}x} + \dfrac{\nu}{1-\nu}\hat{\sigma}_{yy}(x)\right) = \mu\hat{\sigma}_{yx}(x) \\ -\dfrac{2E_0}{1+\nu}\left(\dfrac{\mathrm{d}^2u_y(x)}{\mathrm{d}x^2} - \dfrac{\mathrm{d}\omega_z(x)}{\mathrm{d}x}\right) + \dfrac{\mathrm{d}\hat{\sigma}_{yx}(x)}{\mathrm{d}x} - \beta\left[\dfrac{2E_0}{1+\nu}\left(\dfrac{\mathrm{d}u_y(x)}{\mathrm{d}x} - \omega_z(x)\right) - \hat{\sigma}_{yx}(x)\right] = \mu\hat{\sigma}_{yy}(x) \\ -\dfrac{2E_0\ell^2}{1+\nu}\dfrac{\mathrm{d}^2\omega_z(x)}{\mathrm{d}x^2} - \beta\dfrac{2E_0\ell^2}{1+\nu}\dfrac{\mathrm{d}\omega_z(x)}{\mathrm{d}x} + \dfrac{2E_0}{1+\nu}\omega_z(x) + 2\hat{\sigma}_{yx}(x) - \dfrac{2E_0}{1+\nu}\dfrac{\mathrm{d}u_y(x)}{\mathrm{d}x} = \mu\hat{m}_{yz}(x) \end{cases} \tag{29}$$

We then obtain the general solutions, which are in the form of:

$$\boldsymbol{\Phi} = \sum_{k=1}^{6} \mathrm{e}^{\eta_k x}[\mathcal{A}_k, \mathcal{B}_k, \mathcal{C}_k, \mathcal{D}_k, \mathcal{E}_k, \mathcal{F}_k]^{\mathrm{T}} \tag{30}$$

where $\mathcal{A}_k$, $\mathcal{B}_k$, $\mathcal{C}_k$, $\mathcal{D}_k$, $\mathcal{E}_k$, and $\mathcal{F}_k$ are constants to be determined; η_k are displayed in Appendix A, which are the roots of the following characteristic polynomial established from Eq. (29):

$$\begin{aligned} &\eta^6 + 3\beta\eta^5 + \left[3\left(\beta^2+\mu^2\right) - \frac{1}{\ell^2}\right]\eta^4 + \left[\left(\beta^2+6\mu^2\right) - \frac{2}{\ell^2}\right]\beta\eta^3 \\ &+\left[\beta^2\left(\mu^2\frac{3-2\nu}{1-\nu} - \frac{1}{\ell^2}\right) + \mu^2\left(3\mu^2 - \frac{2}{\ell^2}\right)\right]\eta^2 + \left(\frac{\beta^2\nu}{1-\nu} + 3\mu^2 - \frac{2}{\ell^2}\right)\beta\mu^2\eta \\ &+\frac{\beta^2\mu^2\nu + \mu^4\left(\beta^2\ell^2\nu + \nu - 1\right) + \ell^2\mu^6(1-\nu)}{\ell^2(1-\nu)} = 0 \end{aligned} \tag{31}$$

It is noted that the hexic polynomial is transformed into the cubic equation by replacing η with $\sqrt{\rho} - \beta/2$, and the roots can be solved analytically.

Furthermore, we can further simplify Eq. (29) to explore the relations among the constants above:

$$
\begin{cases}
\dfrac{\mathrm{d}u_x(x)}{\mathrm{d}x}=-\mu\dfrac{1-\nu}{\nu}u_y(x)+\dfrac{(1+\nu)(1-2\nu)}{E_0\nu}\hat{\sigma}_{yy}(x)\\
\dfrac{\mathrm{d}u_y(x)}{\mathrm{d}x}=\mu u_x(x)+2\omega_z(x)\\
\dfrac{\mathrm{d}}{\mathrm{d}x}\left(\dfrac{\mathrm{d}\omega_z(x)}{\mathrm{d}x}+\beta\omega_z(x)\right)=-\dfrac{1}{\ell^2}\left[\mu u_x(x)+\omega_z(x)\right]+\dfrac{1+\nu}{E_0\ell^2}\hat{\sigma}_{yx}(x)-\mu\dfrac{1+\nu}{2E_0\ell^2}\hat{m}_{yz}(x)\\
\dfrac{\mathrm{d}\hat{\sigma}_{yx}(x)}{\mathrm{d}x}=\dfrac{2E_0}{1+\nu}\left[\beta\mu u_x(x)-\mu^2\dfrac{1-\nu}{\nu}u_y(x)+\left(\dfrac{\mathrm{d}\omega_z(x)}{\mathrm{d}x}+\beta\omega_z(x)\right)\right]-\beta\hat{\sigma}_{yx}(x)+\mu\dfrac{2-3\nu}{\nu}\hat{\sigma}_{yy}(x)\\
\dfrac{\mathrm{d}\hat{\sigma}_{yy}(x)}{\mathrm{d}x}=\mu\dfrac{E_0}{1-\nu^2}\left[\mu u_x(x)+\beta u_y(x)+2\omega_z(x)\right]-\mu\dfrac{\nu}{1-\nu}\hat{\sigma}_{yx}(x)-\beta\hat{\sigma}_{yy}(x)\\
\hat{m}_{yz}(x)=\mu\dfrac{2E_0\ell^2}{1+\nu}\omega_z(x)
\end{cases}
\tag{32}
$$

which result in

$$
\begin{cases}
\mathcal{A}_k=\dfrac{(1+\nu)\left[\beta^2\nu+\beta\eta_k+(1-\nu)(\eta_k^2+\mu^2)\right]}{E_0\ell^2\left[\nu(\eta_k(\beta+\eta_k)-\beta\mu+\mu^2)(\beta(\eta_k+\mu)+\eta_k^2+\mu^2)-(\eta_k(\beta+\eta_k)+\mu^2)^2\right]}\mathcal{F}_k\\
\mathcal{B}_k=\dfrac{\nu^2(\mu^2(2\beta+\eta_k)+\eta_k(\beta+\eta_k)^2)-(\beta+\eta_k)\left(\eta_k(\beta+\eta_k)+\mu^2\right)+\beta\mu^2\nu}{E_0\ell^2\mu\left[\nu(\eta_k(\beta+\eta_k)-\beta\mu+\mu^2)(\beta(\eta_k+\mu)+\eta_k^2+\mu^2)-(\eta_k(\beta+\eta_k)+\mu^2)^2\right]}\mathcal{F}_k\\
\mathcal{C}_k=\dfrac{1+\nu}{2E_0\ell^2\mu}\mathcal{F}_k\\
\mathcal{D}_k=\dfrac{(\beta+\eta_k)\left[\nu(\beta+\eta_k)(\eta_k^2+\mu^2)-\eta_k(\eta_k(\beta+\eta_k)+\mu^2)\right]}{\ell^2\mu\left[\nu(\eta_k(\beta+\eta_k)-\beta\mu+\mu^2)(\beta(\eta_k+\mu)+\eta_k^2+\mu^2)-(\eta_k(\beta+\eta_k)+\mu^2)^2\right]}\mathcal{F}_k\\
\mathcal{E}_k=-\dfrac{(\beta+\eta_k)\left[\beta\eta_k+(1-\nu)(\eta_k^2+\mu^2)\right]}{\ell^2\left[\nu(\eta_k(\beta+\eta_k)-\beta\mu+\mu^2)(\beta(\eta_k+\mu)+\eta_k^2+\mu^2)-(\eta_k(\beta+\eta_k)+\mu^2)^2\right]}\mathcal{F}_k
\end{cases}
\tag{33}
$$

Thus, all the constants are represented by $\mathcal{F}_k$ $(k=1,2,\cdots,6)$. The characteristic equation is also derived analytically via the homogeneous boundary conditions:

$$
\begin{vmatrix}
\chi_{11}\mathrm{e}^{\eta_1 L} & \chi_{12}\mathrm{e}^{\eta_2 L} & \chi_{13}\mathrm{e}^{\eta_3 L} & \chi_{14}\mathrm{e}^{\eta_4 L} & \chi_{15}\mathrm{e}^{\eta_5 L} & \chi_{16}\mathrm{e}^{\eta_6 L}\\
\chi_{11}\mathrm{e}^{-\eta_1 L} & \chi_{12}\mathrm{e}^{-\eta_2 L} & \chi_{13}\mathrm{e}^{-\eta_3 L} & \chi_{14}\mathrm{e}^{-\eta_4 L} & \chi_{15}\mathrm{e}^{-\eta_5 L} & \chi_{16}\mathrm{e}^{-\eta_6 L}\\
\chi_{21}\mathrm{e}^{\eta_1 L} & \chi_{22}\mathrm{e}^{\eta_2 L} & \chi_{23}\mathrm{e}^{\eta_3 L} & \chi_{24}\mathrm{e}^{\eta_4 L} & \chi_{25}\mathrm{e}^{\eta_5 L} & \chi_{26}\mathrm{e}^{\eta_6 L}\\
\chi_{21}\mathrm{e}^{-\eta_1 L} & \chi_{22}\mathrm{e}^{-\eta_2 L} & \chi_{23}\mathrm{e}^{-\eta_3 L} & \chi_{24}\mathrm{e}^{-\eta_4 L} & \chi_{25}\mathrm{e}^{-\eta_5 L} & \chi_{26}\mathrm{e}^{-\eta_6 L}\\
\dfrac{\eta_1}{\mu}\mathrm{e}^{\eta_1 L} & \dfrac{\eta_2}{\mu}\mathrm{e}^{\eta_2 L} & \dfrac{\eta_3}{\mu}\mathrm{e}^{\eta_3 L} & \dfrac{\eta_4}{\mu}\mathrm{e}^{\eta_4 L} & \dfrac{\eta_5}{\mu}\mathrm{e}^{\eta_5 L} & \dfrac{\eta_6}{\mu}\mathrm{e}^{\eta_6 L}\\
\dfrac{\eta_1}{\mu}\mathrm{e}^{-\eta_1 L} & \dfrac{\eta_2}{\mu}\mathrm{e}^{-\eta_2 L} & \dfrac{\eta_3}{\mu}\mathrm{e}^{-\eta_3 L} & \dfrac{\eta_4}{\mu}\mathrm{e}^{-\eta_4 L} & \dfrac{\eta_5}{\mu}\mathrm{e}^{-\eta_5 L} & \dfrac{\eta_6}{\mu}\mathrm{e}^{-\eta_6 L}
\end{vmatrix}=0
\tag{34}
$$

where

$$\begin{cases}\chi_{1k}=\dfrac{\mu\left[\beta\eta_k+(1-\nu)(\eta_k^2+\mu^2)\right]}{\ell^2\left[\nu(\eta_k(\beta+\eta_k)-\beta\mu+\mu^2)(\beta(\eta_k+\mu)+\eta_k^2+\mu^2)-(\eta_k(\beta+\eta_k)+\mu^2)^2\right]}\\ \chi_{2k}=\dfrac{\eta_k(\eta_k(\beta+\eta_k)+\mu^2)-\nu(\beta+\eta_k)(\eta_k^2+\mu^2)}{\ell^2\left[\nu(\eta_k(\beta+\eta_k)-\beta\mu+\mu^2)(\beta(\eta_k+\mu)+\eta_k^2+\mu^2)-(\eta_k(\beta+\eta_k)+\mu^2)^2\right]}\end{cases} \tag{35}$$

We then obtain the eigenvalues μ_n from Eq. (34), which lead to the nontrivial solutions of $\mathcal{F}_k$. It is noted that if $\mu_n\in\mathbb{R}$, it might be a multiple eigenvalue, whose eigenvectors are constructed according to

$$\begin{cases}\boldsymbol{\mathcal{H}}\boldsymbol{\Phi}_n^{(0)}=\mu_n\boldsymbol{\Phi}_n^{(0)}\\ \boldsymbol{\mathcal{H}}\boldsymbol{\Phi}_n^{(r+1)}=\mu_n\boldsymbol{\Phi}_n^{(r+1)}+\boldsymbol{\Phi}_n^{(r)}\end{cases}\Rightarrow\left(\boldsymbol{\mathcal{H}}-\mu_n\mathbf{I}_6\right)^{r+1}\boldsymbol{\Phi}_n^{(r)}=0\quad(r=0,1,\cdots,N_n-1) \tag{36}$$

which is further discussed in Appendix B. Hence, the eigen-solutions for general eigenvalues are

$$\boldsymbol{f}_{\mu,n}^{(i)}=\mathrm{e}^{\mu_n y}\left(\boldsymbol{\Phi}_n^{(i)}+y\boldsymbol{\Phi}_n^{(i-1)}+\cdots+\frac{y^i}{i!}\boldsymbol{\Phi}_n^{(0)}\right)\quad(i=0,1,\cdots,N_n) \tag{37}$$

where N_n is the multiplicity. If μ_n is a single eigenvalue (e.g., a certain $\mu_n\in\mathbb{C}\setminus\mathbb{R}$), then $N_n=0$.

2.3. Complete solution

The complete solution for contact analysis consists of the eigen-solutions displayed above for superposition, and the symplectic expansion is

$$\begin{aligned}\tilde{\boldsymbol{f}}&=\boldsymbol{\mathcal{M}}\boldsymbol{f}\\ &=\sum_{n=1}^{6}\gamma_{0,n}\tilde{\boldsymbol{f}}_{0,n}+\sum_{n=1}^{\infty}\sum_{i=0}^{N_n}\left(\gamma_{\mu,n}^{\mathrm{Re},i}\mathrm{Re}\tilde{\boldsymbol{f}}_{\mu,n}^{(i)}+\gamma_{\mu,n}^{\mathrm{Im},i}\mathrm{Im}\tilde{\boldsymbol{f}}_{\mu,n}^{(i)}+\gamma_{-\mu,n}^{\mathrm{Re},i}\mathrm{Re}\tilde{\boldsymbol{f}}_{-\mu,n}^{(i)}+\gamma_{-\mu,n}^{\mathrm{Im},i}\mathrm{Im}\tilde{\boldsymbol{f}}_{-\mu,n}^{(i)}\right)\\ &\equiv\sum_{n=1}^{\infty}\gamma_n\tilde{\boldsymbol{f}}_n\end{aligned} \tag{38}$$

where $\boldsymbol{\mathcal{M}}=\mathrm{diag}[1,1,1,\mathrm{e}^{\beta x},\mathrm{e}^{\beta x},\mathrm{e}^{\beta x}]$; $\tilde{\boldsymbol{f}}_{0,n}$ $(n=1,2,\cdots,6)$ stand for eigen-solutions of zero eigenvalue; $\tilde{\boldsymbol{f}}_{\mu,n}^{(i)}$ and $\tilde{\boldsymbol{f}}_{-\mu,n}^{(i)}$ represent the ith-order eigen-solutions corresponding to the general eigenvalues μ_n and $-\mu_n$, respectively; $\mathrm{Re}(\cdot)$ and $\mathrm{Im}(\cdot)$ are the real and imaginary part of the state vector, respectively; $\gamma_{0,n}$, $\gamma_{\mu,n}^{\mathrm{Re},i}$, $\gamma_{\mu,n}^{\mathrm{Im},i}$, $\gamma_{-\mu,n}^{\mathrm{Re},i}$, $\gamma_{-\mu,n}^{\mathrm{Im},i}$, and γ_n represent the parameters for expansion. The expression exhibited in Eq. (38) indicates that when the eigenvalue is real, the

solution is established according to the first form (the Jordan chain should be considered for the corresponding eigenvectors), whereas if it is complex other than real, the solution should be formulated in accordance with the second form.

Without loss of generality, we assume the boundary conditions at $y=h$ and $y=0$ are

$$y=h,\quad \begin{cases} u_x=0 \\ u_y=0 \\ \omega_z=0 \end{cases};\quad y=0,\quad \begin{cases} u_y=d & x\in[a,b] \\ u_x=0 & x\in[a,b] \\ \omega_z=0 & x\in[a,b] \\ \sigma_{yy}=0 & x\in[-L,a]\cup[b,L] \\ \sigma_{yx}=0 & x\in[-L,a]\cup[b,L] \\ m_{yz}=0 & x\in[-L,a]\cup[b,L] \end{cases} \tag{39}$$

where d is the maximum indentation depth, which reflects the indenter shape; $x\in[a,b]$ is the contact area. It is noted that Eq. (40) are the boundary conditions of the sticking (no-slip) indentation for a finite-sized plane, rather than half-plane [26]. To solve for the mixed boundary-value problem, the Hamiltonian mixed energy variational principal reads [27]

$$\begin{aligned} &\delta\left\{\int_0^h\int_{-L}^{L}\left[\boldsymbol{p}^{\mathrm{T}}\frac{\partial \boldsymbol{q}}{\partial y}-H(\boldsymbol{q},\boldsymbol{p})\right]\mathrm{d}x\mathrm{d}y-\int_{\Gamma_{\boldsymbol{q}_h}}\left[\boldsymbol{p}^{\mathrm{T}}(\boldsymbol{q}-\overline{\boldsymbol{q}}_h)\right]\mathrm{d}x\right. \\ &\left.-\int_{\Gamma_{\boldsymbol{p}_h}}\left[\overline{\boldsymbol{p}}_h{}^{\mathrm{T}}\boldsymbol{q}\right]\mathrm{d}x+\int_{\Gamma_{\boldsymbol{q}_0}}\left[\boldsymbol{p}^{\mathrm{T}}(\boldsymbol{q}-\overline{\boldsymbol{q}}_0)\right]\mathrm{d}x+\int_{\Gamma_{\boldsymbol{p}_0}}\left[\overline{\boldsymbol{p}}_0{}^{\mathrm{T}}\boldsymbol{q}\right]\mathrm{d}x\right\}=0 \end{aligned} \tag{40}$$

Then, Eq. (41) can be further simplified to

$$\begin{aligned} &\int_{\Gamma_{\boldsymbol{p}_h}}\left[(\delta\boldsymbol{q})^{\mathrm{T}}(\boldsymbol{p}-\overline{\boldsymbol{p}}_h)\right]\mathrm{d}x-\int_{\Gamma_{\boldsymbol{q}_h}}\left[(\delta\boldsymbol{p})^{\mathrm{T}}(\boldsymbol{q}-\overline{\boldsymbol{q}}_h)\right]\mathrm{d}x \\ &+\int_{\Gamma_{\boldsymbol{q}_0}}\left[(\delta\boldsymbol{p})^{\mathrm{T}}(\boldsymbol{q}-\overline{\boldsymbol{q}}_0)\right]\mathrm{d}x-\int_{\Gamma_{\boldsymbol{p}_0}}\left[(\delta\boldsymbol{q})^{\mathrm{T}}(\boldsymbol{p}-\overline{\boldsymbol{p}}_0)\right]\mathrm{d}x=0 \end{aligned} \tag{41}$$

for the displacements and stresses satisfy the canonical equation within the contact area. Substituting Eq. (38) into Eq. (42), we have

$$\begin{aligned} &\int_{\Gamma_{\boldsymbol{p}_h}}\left[(\sum_{i=1}^{\infty}\delta\gamma_n\boldsymbol{q}_n)^{\mathrm{T}}(\sum_{j=1}^{\infty}\gamma_m\boldsymbol{p}_m-\overline{\boldsymbol{p}}_h)\right]\mathrm{d}x-\int_{\Gamma_{\boldsymbol{q}_h}}\left[(\sum_{i=1}^{\infty}\delta\gamma_n\boldsymbol{p}_n)^{\mathrm{T}}(\sum_{j=1}^{\infty}\gamma_m\boldsymbol{q}_m-\overline{\boldsymbol{q}}_h)\right]\mathrm{d}x \\ &+\int_{\Gamma_{\boldsymbol{q}_0}}\left[(\sum_{i=1}^{\infty}\delta\gamma_n\boldsymbol{p}_n)^{\mathrm{T}}(\sum_{j=1}^{\infty}\gamma_m\boldsymbol{q}_m-\overline{\boldsymbol{q}}_0)\right]\mathrm{d}x-\int_{\Gamma_{\boldsymbol{p}_0}}\left[(\sum_{i=1}^{\infty}\delta\gamma_n\boldsymbol{q}_n)^{\mathrm{T}}(\sum_{j=1}^{\infty}\gamma_m\boldsymbol{p}_m-\overline{\boldsymbol{p}}_0)\right]\mathrm{d}x=0 \end{aligned} \tag{42}$$

On letting

$$\begin{aligned}\Theta_{nm} &= \int_{\Gamma_{p_h}} \left[(\boldsymbol{q}_n)^{\mathrm{T}} \boldsymbol{p}_m\right] \mathrm{d}x - \int_{\Gamma_{q_h}} \left[(\boldsymbol{p}_n)^{\mathrm{T}} \boldsymbol{q}_m\right] \mathrm{d}x + \int_{\Gamma_{q_0}} \left[(\boldsymbol{p}_n)^{\mathrm{T}} \boldsymbol{q}_m\right] \mathrm{d}x - \int_{\Gamma_{p_0}} \left[(\boldsymbol{q}_n)^{\mathrm{T}} \boldsymbol{p}_m\right] \mathrm{d}x \\ \Omega_n &= \int_{\Gamma_{p_h}} \left[(\boldsymbol{q}_n)^{\mathrm{T}} \overline{\boldsymbol{p}}_h\right] \mathrm{d}x - \int_{\Gamma_{q_h}} \left[(\boldsymbol{p}_n)^{\mathrm{T}} \overline{\boldsymbol{q}}_h\right] \mathrm{d}x + \int_{\Gamma_{q_0}} \left[(\boldsymbol{p}_n)^{\mathrm{T}} \overline{\boldsymbol{q}}_0\right] \mathrm{d}x - \int_{\Gamma_{p_0}} \left[(\boldsymbol{q}_n)^{\mathrm{T}} \overline{\boldsymbol{p}}_0\right] \mathrm{d}x \end{aligned} \tag{43}$$

Eq. (43) may be rewritten as

$$\Theta_{nm} \gamma_m = \Omega_n \tag{44}$$

If Eq. (45) is compatible, the result is in the form of

$$\gamma_i = \frac{\det \Theta_{nm}^i}{\det \Theta_{nm}} \tag{45}$$

where Θ_{nm}^i represents the matrix formed by replacing the i-th column of Θ_{nm} by the column vector Ω_n.

3. Analysis and discussion

3.1. Distributions of eigenvalues and local phase transition

The determination of the form for eigen-solutions is generally linked to the distribution of eigenvalues, thereby necessitating an analysis of the patterns. The length and width of a plane are set as $2L$ and h, respectively. The Young's modulus is assumed to vary exponentially as $E_0 \mathrm{e}^{\beta x}$, while Poisson's ratio ν keeps constant. ℓ is material characteristic length. In addition, the lateral boundaries are chosen to be fixed, i.e., $u_x(\pm L) = 0$, $u_y(\pm L) = 0$, and $\omega_z(\pm L) = 0$.

To elucidate the size effect, we may let $E_0 = 1$ (MPa), $\beta = 0.1$ (mm^{-1}), $\nu = 0.25$, $h = 10$ (mm), and $\ell = 0.01$ (mm), then the distributions of eigenvalues are as follows with distinct L:

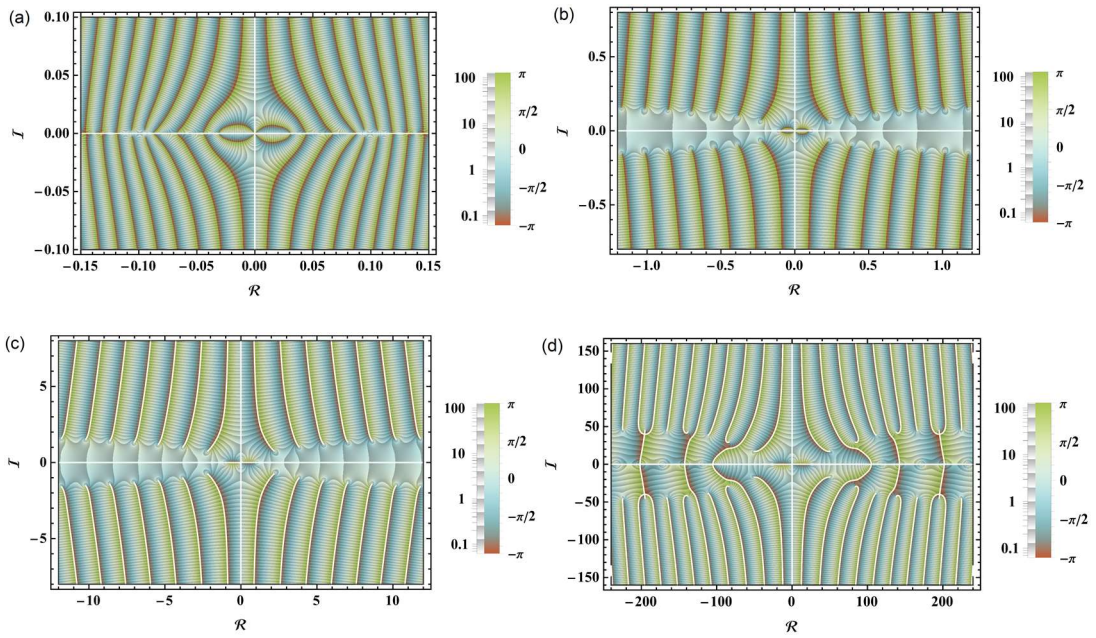

Fig. 2. Distributions of eigenvalues at different lengths. (a) $L = 100$ (mm) (b) $L = 10$ (mm) (c) $L = 1$ (mm) (d) $L = 0.05$ (mm)

It is noteworthy that the distributions of eigenvalues remain quasi self-similar within a certain range, which are displayed in Fig. 2 (b) and (c). As the lengths of the specimen diminish, the local phase transitions occur, which is a consequence of the size effect. Specifically, we observe that the eigenvalues are partially real rather than complex, shown in Fig. 2(d), which leads to intriguing phenomena, e.g., the absence of the stress concentration at the corners. It is observable that as L decreases, the distance between the symplectic adjoint eigenvalues and their complex conjugate counterparts along the imaginary axis progressively widens. Notably, at $L = 100$ (mm) in Fig. 2(a), these two sets of eigenvalues gather to a nearly overlapping state, then separate again away from the coordinate origin. Actually, real eigenvalues also emerge in eigenmodes of high order (far away from the coordinate origin) for the case with large L, whereas no real eigenvalue is present in the initial few eigenmodes that have a significant impact on the eigen-solutions (close to the coordinate origin), which is the concept of "local" in the local phase

transition.

3.2. Numerical example

Consider a no-slip contact model: a rigid flat punch is applied on the surface of an exponentially graded plane in the x-direction, the length and width of which are $2L=2$ (m) and $h=1$ (m) respectively. The Young's modulus at the coordinate origin, material gradient index, Poisson's ratio, and material characteristic length are chosen to be $E_0=1$ (Pa), $\beta=0.1$ (m^{-1}), $\nu=0.25$, and $\ell=0.01$ (m), respectively. The lateral boundary conditions are assumed to be homogeneous: $u_x(\pm L)=0$, $u_y(\pm L)=0$, and $\omega_z(\pm L)=0$, while the boundary conditions at $y=h$ and $y=0$ are taken as Eq. (40), wherein $a=0.2$ (m), $b=0.3$ (m), and $d=0.02$ (m).

As an illustrative example, we present the results pertaining to displacements, rotation vectors, stresses, and couple stresses:

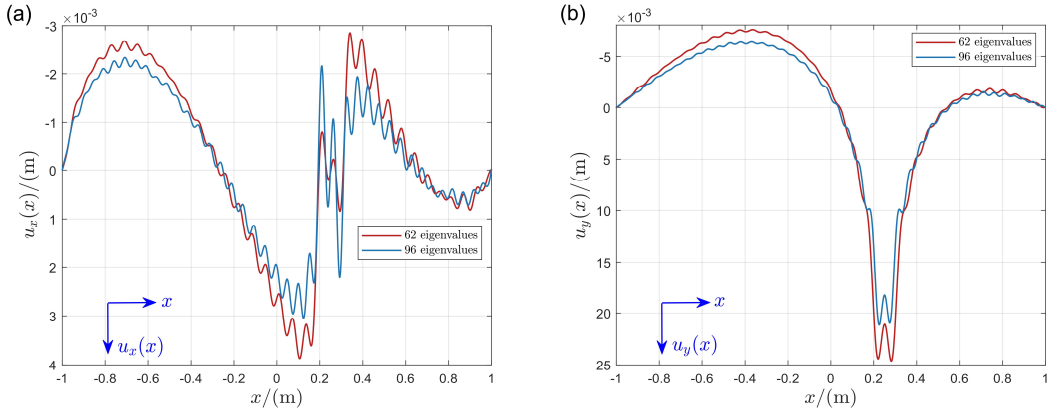

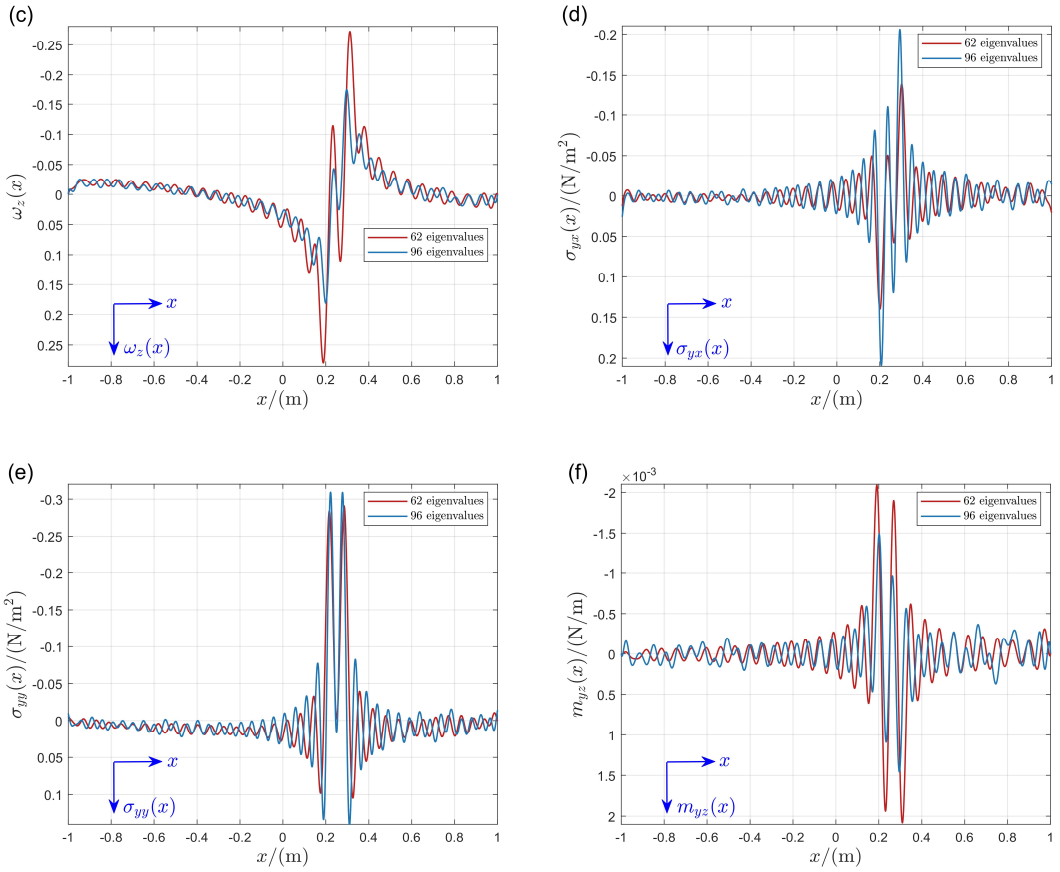

Fig. 3. Examples of symplectic solutions for displacements, rotation vectors, stresses, and couple stresses. (a) u_x (b) u_y (c) ω_z (d) σ_{yx} (e) σ_{yy} (f) m_{yz}

It is noteworthy that 62 eigenvalues are involved to obtain the first analytical solution in comparation with the second result, since the real eigenvalues emerge when $\Re(\mu)>100$ (i.e., the 63$^{\mathrm{rd}}$ eigenvalue is the first real eigenvalue), as depicted in Fig. 4. To clarify, the real eigenvalues may be the multi-zeros of the characteristic equation, which may lead to the consideration of Jordan chain in the construction of the eigen-solutions. Given the fixed lateral boundaries, we have noticed the displacements at $x=\pm L$ remain zero, while the stresses are nonzero, as illustrated in Fig. 3. Besides, the shear stress and couple stress are nonzero compared with the results derived from the case of frictionless punches. However, the horizontal

displacement and the rotation vector keep zero due to the no-slip condition. The oscillating behavior is caused by the superposition of a finite number of eigen-solutions, and the consequence will converge with the involvement of adequate eigenvalues.

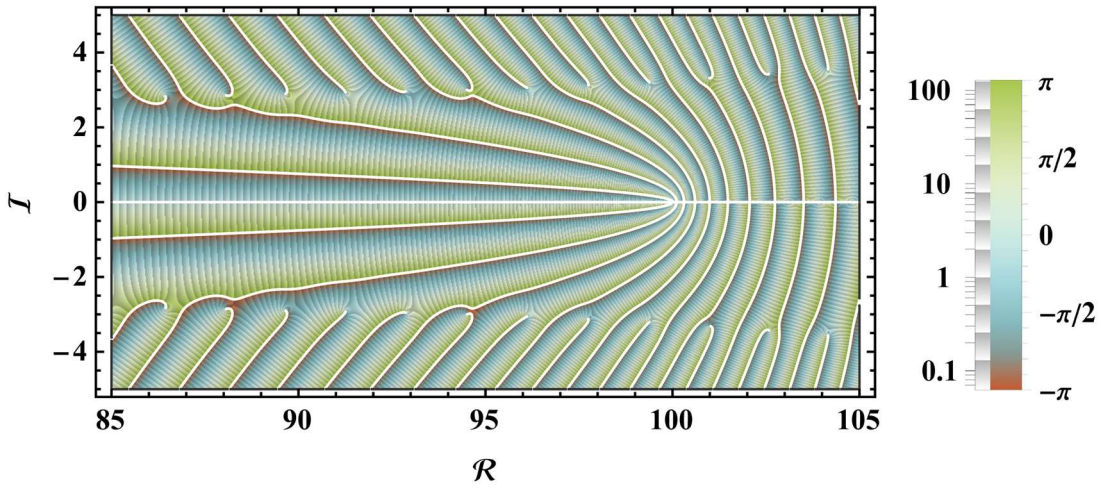

Fig. 4. Critical region where real eigenvalues emerge. (real axis $\Re(\mu)\in[85,105]$ and imaginary axis $\Im(\mu)\in[-5,5]$)

4. Conclusions

We have established a novel symplectic framework for the couple stress theory, which is suitable for contact analysis. The contact between a no-slip rigid punch and a finite-sized plane with horizontal exponential material gradient is analyzed. Upon transforming the governing equations into the symplectic form, we obtain a new quasi-Hamiltonian operator, the lower-left block of which is symmetry breaking. To explain, the "symmetry breaking" arises from the inherent asymmetric stress tensors. Furthermore, the dual Hamiltonian transformation is derived, with all the eigen-solutions constructed analytically, which are substituted into the symplectic expansion subsequently. It is worth noting that the properties of the eigenvalues should be determined beforehand, resulting in the derivation of the coefficients for superposition in distinct forms.

The local phase transition is investigated in the analysis for the distributions of the eigenvalues. The existence of real eigenvalues offers a rationale for the phenomenon of size effect. Additionally, the numerical example is conducted with a no-slip rigid flat punch acting on a finite-sized graded plane. The symplectic methodology not only offers a powerful tool but also ushers in new possibilities for deeper understanding and innovative solutions to complicated contact analysis, forging a solid foundation and for subsequent investigations and advancements.

Acknowledgments

The work was supported by the National Natural Science Foundation of China (Nos. 12192211 and 12192210), the Natural Science Foundation of Zhejiang Province (No. LD21A020001), and the 111 Project, PR China (No. B21034). This work was also partly supported by the specialized research projects of Huanjiang Laboratory, Zhuji, Zhejiang Province.

References

[1] E. C. Aifantis, Gradient effects at macro, micro, and nano scales, J. Mech. Behav. Biomed. Mater., vol. 5, no. 3, pp. 355–375, 1994, DOI: 10.1515/JMBM.1994.5.3.355.

[2] E. Broitman, The nature of the frictional force at the macro-, micro-, and nano-scales, Friction, vol. 2, no. 1, pp. 40–46, Mar. 2014, DOI: 10.1007/s40544-014-0037-3.

[3] J. W. Judy, Microelectromechanical systems (MEMS): fabrication, design and applications, Smart. Mater. Struct., vol. 10, no. 6, p. 1115, 2001, DOI: 10.1088/0964-1726/10/6/301.

[4] C. Morrow, M. Lovell, and X. Ning, A JKR–DMT transition solution for adhesive rough surface contact, J. Phys. D Appl. Phys., vol. 36, no. 5, p. 534, 2003, DOI: 10.1088/0022-

3727/36/5/317.

[5] R. Toupin, Elastic materials with couple-stresses, Arch. Ration. Mech. Anal., vol. 11, no. 1, pp. 385–414, 1962, DOI: 10.1007/BF00253945.

[6] R. D. Mindlin and H. Tiersten, Effects of couple-stresses in linear elasticity, Arch. Ration. Mech. Anal., vol. 11, pp. 415–448, 1962, DOI: 10.1007/BF00253946.

[7] W. Koiter, Couple-stresses in the theory of elasticity, I & II, Proc. K. Ned. Akad. Wet. Ser. B, vol. 67, pp. 17–44, 1969.

[8] E. Kröner, Elasticity theory of materials with long range cohesive forces, Int. J. Solids Struct., vol. 3, no. 5, pp. 731–742, 1967, DOI: 10.1016/0020-7683(67)90049-2.

[9] H.-T. Thai, T. P. Vo, T.-K. Nguyen, and S.-E. Kim, A review of continuum mechanics models for size-dependent analysis of beams and plates, Compos. Struct., vol. 177, pp. 196–219, Oct. 2017, DOI: 10.1016/j.compstruct.2017.06.040.

[10] F. Yang, A. C. M. Chong, D. C. C. Lam, and P. Tong, Couple stress based strain gradient theory for elasticity, Int. J. Solids Struct., vol. 39, no. 10, pp. 2731–2743, May 2002, DOI: 10.1016/S0020-7683(02)00152-X.

[11] R. Muki and E. Sternberg, The influence of couple-stresses on singular stress concentrations in elastic solids, Z. Angew. Math. Phys, vol. 16, no. 5, pp. 611–648, Sep. 1965, DOI: 10.1007/BF01590966.

[12] T. Zisis, Some basic contact problems in couple stress elasticity, Int. J. Solids Struct., vol. 51, pp. 2084–2095, 2014, DOI: 10.1016/j.ijsolstr.2014.02.016.

[13] P. A. Gourgiotis, Th. Zisis, and K. P. Baxevanakis, Analysis of the tilted flat punch in couple-stress elasticity, Int. J. Solids Struct., vol. 85–86, pp. 34–43, May 2016, DOI:

10.1016/j.ijsolstr.2016.01.017.

[14] P. Gourgiotis and T. Zisis, Two-dimensional indentation of microstructured solids characterized by couple-stress elasticity, J. Strain Anal. Eng. Des., vol. 51, no. 4, pp. 318–331, 2016, DOI: 10.1177/0309324715611524.

[15] T. Zisis, Anti-plane loading of microstructured materials in the context of couple stress theory of elasticity: half-planes and layers, Arch. Appl. Mech., vol. 88, no. 1–2, pp. 97–110, Feb. 2018, DOI: 10.1007/s00419-017-1277-2.

[16] T. Zisis, Burmister's problem extended to a microstructuredlayer, J. Mech. Mater. Struct., vol. 13, no. 2, pp. 203–223, May 2018, DOI: 10.2140/jomms.2018.13.203.

[17] T. Zisis, P. Gourgiotis, and F. Dal Corso, A contact problem in couple stress thermoelasticity: the indentation by a hot flat punch, Int. J. Solids Struct., vol. 63, pp. 226–239, 2015, DOI: 10.1016/j.ijsolstr.2015.03.002.

[18] Y. Wang, X. Zhang, H. Shen, J. Liu, and B. Zhang, Couple stress-based 3D contact of elastic films, Int. J. Solids Struct., vol. 191–192, pp. 449–463, May 2020, DOI: 10.1016/j.ijsolstr.2020.01.005.

[19] Y. Wang, X. Zhang, H. Shen, J. Liu, B. Zhang, and S. Xu, Three-dimensional contact analysis with couple stress elasticity, Int. J. Mech. Sci., vol. 153–154, pp. 369–379, Apr. 2019, DOI: 10.1016/j.ijmecsci.2019.02.016.

[20] C. A. Clifford and M. Seah, Modelling of nanomechanical nanoindentation measurements using an AFM or nanoindenter for compliant layers on stiffer substrates, Nanotechnology, vol. 17, no. 21, p. 5283, 2006, DOI: 10.1088/0957-4484/17/21/001.

[21] N. E. Kurland, Z. Drira, and V. K. Yadavalli, Measurement of nanomechanical properties

of biomolecules using atomic force microscopy, Micron, vol. 43, no. 2–3, pp. 116–128, Feb. 2012, DOI: 10.1016/j.micron.2011.07.017.

[22] H.-X. Song, L.-L. Ke, and Y.-S. Wang, Sliding frictional contact analysis of an elastic solid with couple stresses, Int. J. Mech. Sci., vol. 133, pp. 804–816, Nov. 2017, DOI: 10.1016/j.ijmecsci.2017.09.037.

[23] W.-X. Zhong, A new systematic methodology for theory of elasticity. Dalian: Dalian University of Technology Press, 1995. (in Chinese)

[24] W. Yao, W. Zhong, and C. W. Lim, Symplectic elasticity. New Jersey: World Scientific, 2009.

[25] W. X. Zhong, G.-X. Fang, and W.-A. Yao, Symplectic solution for a plane couple stress problem, Adv. Mat. Res., vol. 9, pp. 143–152, 2005, DOI: 10.4028/www.scientific.net/AMR.9.143.

[26] I. Argatov and G. Mishuris, Indentation testing of biological materials, vol. 91. Springer, 2018.

[27] A. Y. T. Leung and J. Zheng, Closed form stress distribution in 2D elasticity for all boundary conditions, Appl. Math. Mech.-Engl. Ed., vol. 28, no. 12, pp. 1629–1642, Dec. 2007, DOI: 10.1007/s10483-007-1210-z.

Appendix A

The roots deduced from Eq. (31) are in the form of

$$\begin{aligned}
\eta_1 &= \frac{1}{2}\left[-\beta-\sqrt{\beta^2-4\left(\varpi_1+\varpi_2+\varpi_3\right)}\right], & \eta_4 &= \frac{1}{2}\left[-\beta+\sqrt{\beta^2-4\left(\varpi_1+\varpi_2+\varpi_3\right)}\right] \\
\eta_2 &= \frac{1}{2}\left[-\beta-\sqrt{\beta^2-4\left(\varpi_1-\frac{1-\mathrm{i}\sqrt{3}}{2}\varpi_2-\frac{1+\mathrm{i}\sqrt{3}}{2}\varpi_3\right)}\right], & \eta_5 &= \frac{1}{2}\left[-\beta+\sqrt{\beta^2-4\left(\varpi_1-\frac{1-\mathrm{i}\sqrt{3}}{2}\varpi_2-\frac{1+\mathrm{i}\sqrt{3}}{2}\varpi_3\right)}\right] \\
\eta_3 &= \frac{1}{2}\left[-\beta-\sqrt{\beta^2-4\left(\varpi_1-\frac{1+\mathrm{i}\sqrt{3}}{2}\varpi_2-\frac{1-\mathrm{i}\sqrt{3}}{2}\varpi_3\right)}\right], & \eta_6 &= \frac{1}{2}\left[-\beta+\sqrt{\beta^2-4\left(\varpi_1-\frac{1+\mathrm{i}\sqrt{3}}{2}\varpi_2-\frac{1-\mathrm{i}\sqrt{3}}{2}\varpi_3\right)}\right]
\end{aligned} \tag{A.1}$$

where

$$\begin{aligned}
\varpi_1 &= \mu^2-\frac{1}{3\ell^2} \\
\varpi_2 &= \frac{\Xi}{3(1-\nu)} \\
\varpi_3 &= \frac{1-\nu-3\ell^4\beta^2\mu^2\nu}{3\ell^4\Xi} \\
\Xi &= \sqrt[3]{\nu^3\left(18\beta^2\mu^2\ell^4+1\right)-3\nu^2\left(12\beta^2\mu^2\ell^4+1\right)+3\nu\left(6\beta^2\mu^2\ell^4+1\right)+3\sqrt{3}\ell^2\sqrt{\beta^2\mu^2(1-\nu)^3\nu\left(\nu\left(11\beta^2\mu^2\ell^4+2\right)+\nu^2\left(\beta^4\mu^4\ell^8-11\beta^2\mu^2\ell^4-1\right)-1\right)-1}}\Big/\ell^2
\end{aligned} \tag{A.2}$$

Appendix B

Take $N_n=2$ for instance (i.e., the multiplicity of μ_n is 3), Eq. (36) is simplified to

$$\begin{cases} \boldsymbol{\mathcal{H}}\boldsymbol{\Phi}_n^{(0)} = \mu_n \boldsymbol{\Phi}_n^{(0)} \\ \boldsymbol{\mathcal{H}}\boldsymbol{\Phi}_n^{(1)} = \mu_n \boldsymbol{\Phi}_n^{(1)} + \boldsymbol{\Phi}_n^{(0)} \\ \boldsymbol{\mathcal{H}}\boldsymbol{\Phi}_n^{(2)} = \mu_n \boldsymbol{\Phi}_n^{(2)} + \boldsymbol{\Phi}_n^{(1)} \end{cases} \tag{B.1}$$

The last two equations in Eq. (B.1) are usually solved via the variation of the constants method. Given that the eigenvectors are non-zero, we may further assume evolution matrices $\boldsymbol{Q}_n^{(1)}$ and $\boldsymbol{Q}_n^{(2)}$ that fulfill:

$$\begin{cases} \boldsymbol{\Phi}_n^{(1)} = \boldsymbol{Q}_n^{(1)} \boldsymbol{\Phi}_n^{(0)} \\ \boldsymbol{\Phi}_n^{(2)} = \boldsymbol{Q}_n^{(2)} \boldsymbol{\Phi}_n^{(1)} \end{cases} \tag{B.2}$$

the properties of which are obtained through modifying the first and last two formulas respectively in Eq. (B.1) as

$$\begin{cases} \boldsymbol{Q}_n^{(1)} \boldsymbol{\mathcal{H}} \boldsymbol{\Phi}_n^{(0)} = \mu_n \boldsymbol{Q}_n^{(1)} \boldsymbol{\Phi}_n^{(0)} \\ \boldsymbol{\mathcal{H}} \boldsymbol{Q}_n^{(1)} \boldsymbol{\Phi}_n^{(0)} = \mu_n \boldsymbol{Q}_n^{(1)} \boldsymbol{\Phi}_n^{(0)} + \boldsymbol{\Phi}_n^{(0)} \end{cases} \tag{B.3}$$

and

$$\begin{cases} \boldsymbol{Q}_n^{(2)} \left(\boldsymbol{\mathcal{H}} - \mu_n \mathbf{I}_6 \right) \boldsymbol{\Phi}_n^{(1)} = \boldsymbol{Q}_n^{(2)} \boldsymbol{\Phi}_n^{(0)} \\ \left(\boldsymbol{\mathcal{H}} - \mu_n \mathbf{I}_6 \right) \boldsymbol{Q}_n^{(2)} \boldsymbol{\Phi}_n^{(1)} = \boldsymbol{\Phi}_n^{(1)} \end{cases} \tag{B.4}$$

from Eq. (B.3) we have an identity

$$\left(\left[\!\left[\boldsymbol{\mathcal{H}}, \boldsymbol{Q}_n^{(1)} \right]\!\right] - \mathbf{I}_6 \right) \boldsymbol{\Phi}_n^{(0)} = 0 \tag{B.5}$$

where $\left[\!\left[\boldsymbol{\mathcal{H}}, \boldsymbol{Q}_n^{(1)}\right]\!\right] = \boldsymbol{\mathcal{H}}\boldsymbol{Q}_n^{(1)} - \boldsymbol{Q}_n^{(1)}\boldsymbol{\mathcal{H}}$ is a commutator.

$$\left[\!\left[\left(\boldsymbol{\mathcal{H}} - \mu_n \mathbf{I}_6\right), \boldsymbol{Q}_n^{(2)}\right]\!\right]\boldsymbol{\Phi}_n^{(1)} = \left(\boldsymbol{Q}_n^{(1)} - \boldsymbol{Q}_n^{(2)}\right)\boldsymbol{\Phi}_n^{(0)} \tag{B.6}$$

is another identity derived from Eq. (B.4).